

Experimental Characterization of Commercially Practical Magnetorheological Fluid Damper Technology

Sean P. Kelso
CSA Engineering
1300 Britt Street SE, Suite 201, Albuquerque, New Mexico

**SPIE Conference on Smart Structures and Materials
Industrial and Commercial Applications of
Smart Structures Technologies**

**San Diego, CA
March 2001**

Paper #4332-34

Copyright 2001 Society of Photo-Optical Instrumentation Engineers. This paper was published in the Proceedings of SPIE Volume 4332-34, Smart Structures and Materials, Industrial and Commercial Applications of Smart Structures Technologies 2001, and is made available as an electronic reprint (preprint) with permission of SPIE. One print or electronic copy may be made for personal use only. Systematic or multiple reproduction, distribution to multiple locations via electronic or other means, duplication of any material in this paper for a fee or for commercial purposes, or modification of the content of the paper are prohibited.

Experimental Characterization of Commercially Practical Magnetorheological Fluid Damper Technology

Shawn P. Kelso*
CSA Engineering, Inc.

ABSTRACT

As technologies for magnetorheological (MR) fluid hardware further evolve towards commercial adoption, the appeal for simpler, more cost-effective solutions becomes evident. While the skills involved in methods of manufacturing and cost-reduction efforts for mass production lie with the manufacturing community, practical and cost-effective MR technologies must first exist. As part of a 'whole approach' MR solution, the MR damper technology presented in this paper illustrates the development of a fast-response, low-power, cost-effective solution. Fundamentally, a competitive 'whole approach' active or semi-active MR solution can be viewed as system of separate components: parameter sensing, intelligent control, power delivery, and MR hardware technology. The development of any one single component should not successfully evolve without the addressing the cost efficiency and commercialization concerns of the other three. The MR hardware component should be predictable in performance behavior, capable of high damping force at minimal power, and fast in time response to complement simplified control schemes. The design effort is further challenged to meet these requirements within a simple, cost-effective package that holds commercial development appeal.

This research includes the characterization of a new prototype MR damper including a description of the device technology, characterization test results and current work. It is evident by these results that this MR technology, comprising simple, commercial-off-the-shelf (COTS) components where possible, presents an attractive, practical and cost effective component of the 'whole approach' MR solution.

Keywords: Magnetorheological fluid, semi-active, controllable, damping, damper, commercialization

INTRODUCTION

As an effort to increase awareness of the benefits and potential commercial viability of magnetorheological (MR) fluid technologies, a new MR fluid damper has been developed at CSA Engineering. This device provides engineers in both MR and non-MR disciplines with a versatile tool that demonstrates the performance capabilities of a fast-response MR damper. Benefits of this design include adjustable zero-field damping, use of commercially available seals and components, an optimized electromagnetic circuit, and ease of serviceability.

The intent of this technology is to address a wide range of research applications. While the response time of the damper has been developed for the physical expression of feedback control schemes, the minimal electrical resistance of the electromagnetic circuit benefits applications where issues such as power consumption and heating are paramount. Characterization testing of multiple physical parameters is also eased with this design, as it can be easily disassembled and re-assembled for fluid or MR-gap height changes. Fine-tuning zero-field or passive damping can be varied across a great range simply by adding or subtracting washer-type shims.

The fundamental concept of this MR damper is to provide a wide range of fast, controllable damping in order to fully utilize the performance benefits offered by controllable viscosity MR fluids. Characterization testing of the damper with different fluids was performed. In this work, a description of the technology is discussed and experimental test results of this new MR damper are presented.

* sk@csaengineering.com; phone 1 505 765 5865; fax 1 505 765 5863; <http://www.csaengineering.com>; CSA Engineering, Inc., 2021 Girard SE #112, Albuquerque, NM 87106

DESCRIPTION OF TECHNOLOGY

While the primary technological contribution of this design lies in the unique flow port and coil configurations of the piston, the entire MR damper development effort was focused on minimal cost and simplicity of design. Several parameters were addressed in the development of this technology. These parameters include:

- Materials of Construction of piston, cylinder and piston shaft
- Commercial, off-the-shelf (COTS) components
- Serviceability and Maintenance
- Zero-Field Damping Adjustment

The engineering prototype expression of this technology is shown in Figure 1. This MR device consists of a piston-cylinder damper and satellite accumulator. The accumulator is separate from the damper cylinder body in this development model to simplify frequent rebuilds. The accumulator cylinder contains a floating piston that separates the compressed nitrogen gas from the MR fluid. The accumulator utilizes a Schraeder valve for pressurization.

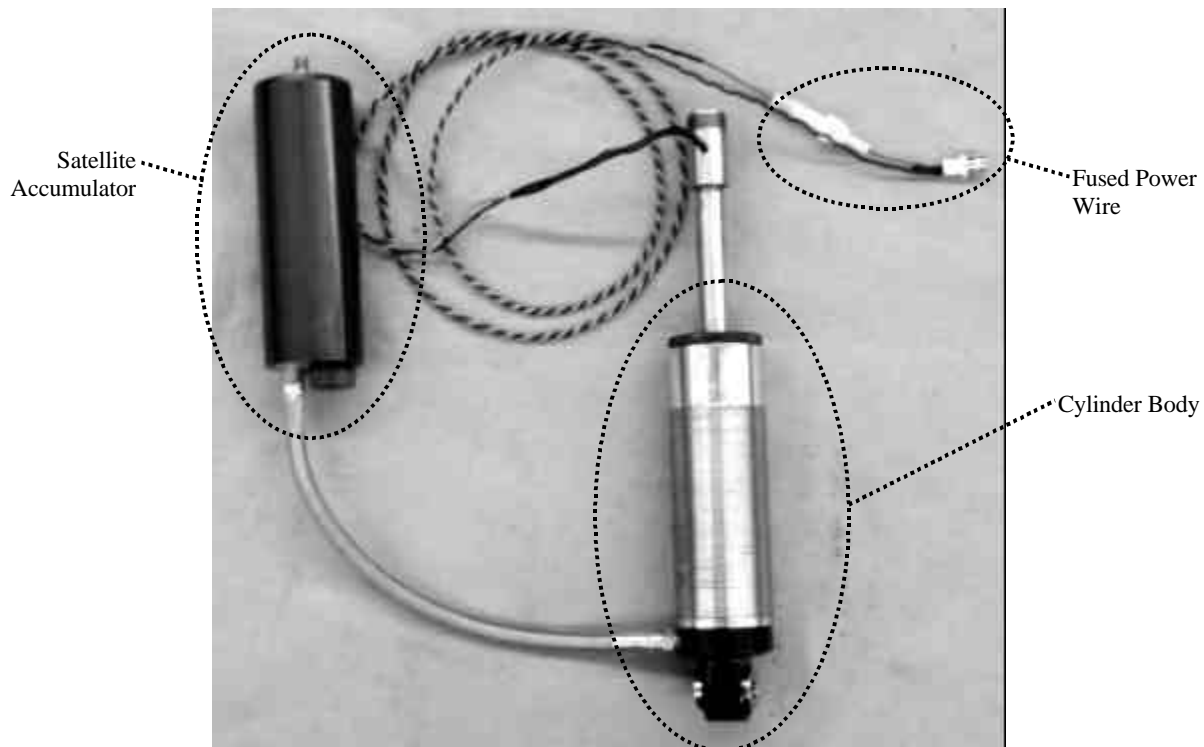


Figure 1 Photo of the engineering prototype MR damper used for testing and characterization

The cylinder body is constructed of non-ferrous stainless steel, as is the piston shaft. The change in *apparent viscosity* [1, 3, 8] of the MR fluid, the source of controllable damping, occurs within the confines of the piston. As such, the electromagnet is integral to the piston and supply wires for the electromagnetic coil exit the damper at the far end of the piston shaft. The piston utilizes a brass-filled PTFE (Teflon) piston seal for dynamic interface with the cylinder, typical to those found in commercial hydraulic shock absorbers. A benefit of this arrangement is that the majority of wear resulting from piston-cylinder reciprocation occurs at the seal and is easily and inexpensively replaced. Seal wear does not adversely affect the MR-effect throughout the seal's life cycle as the fluid orifice and MR-gap are within the body of the piston, internal to the seal.

The piston shaft seal set consists of an external wiper seal, an internal oil seal, and a brass-filled Teflon guide bearing to ensure even loading about the seals. A 15 μ m finish was applied to the piston shaft in order to maintain lubrication of the seals

for maximum operation between servicing [7]. Remaining internal static seals are O-rings. All seals, O-rings and guide bearings are commercially available in commonly found sizes.

As this MR damper was designed to serve several different research applications and potentially diverse damping environments, performance versatility was a paramount concern during the design phase. Performance versatility is achieved by providing the ability to vary and fine-tune zero-field damping performance. Zero-field damping behavior is defined as the passive damping force delivered by the device in the absence of electric current. In this mode, MR fluid and hydraulic fluid dampers are similar in that damping force is a function of orifice geometry and fluid viscosity [3, 4, 7, 8]. The fluid orifice size, which is also the MR-gap for this damper design, is determined by the stack height of shim washers inserted into the piston. Changing the shim height can be performed without removal or disassembly of the damper's electromagnetic circuit.

Two separate damping cases were investigated to illustrate the differences in damping resulting solely from different MR-gap heights. Dynamic damping force range data for one frequency/amplitude data point is shown in Figure 2. In this graph, average peak damping force for the MR damper at zero-field with a 0.065" gap is 31.2lbf. With a 0.035" gap, average peak damping force increased to 116.5lbf. It should be noted that the ratio of damping force between 0.0A to 6.0A with the 0.035" gap is approximately 6.2:1, while the larger 0.065" gap produced a ratio of 4.6:1. For the range of frequencies and amplitudes tested (0.5Hz to 4Hz & 0.13" to 0.5" peak amplitude), the aforementioned ratio ranged from 11:1 to 3.1:1 for the smaller gap, and 9:1 to 4.2:1 for the larger gap.

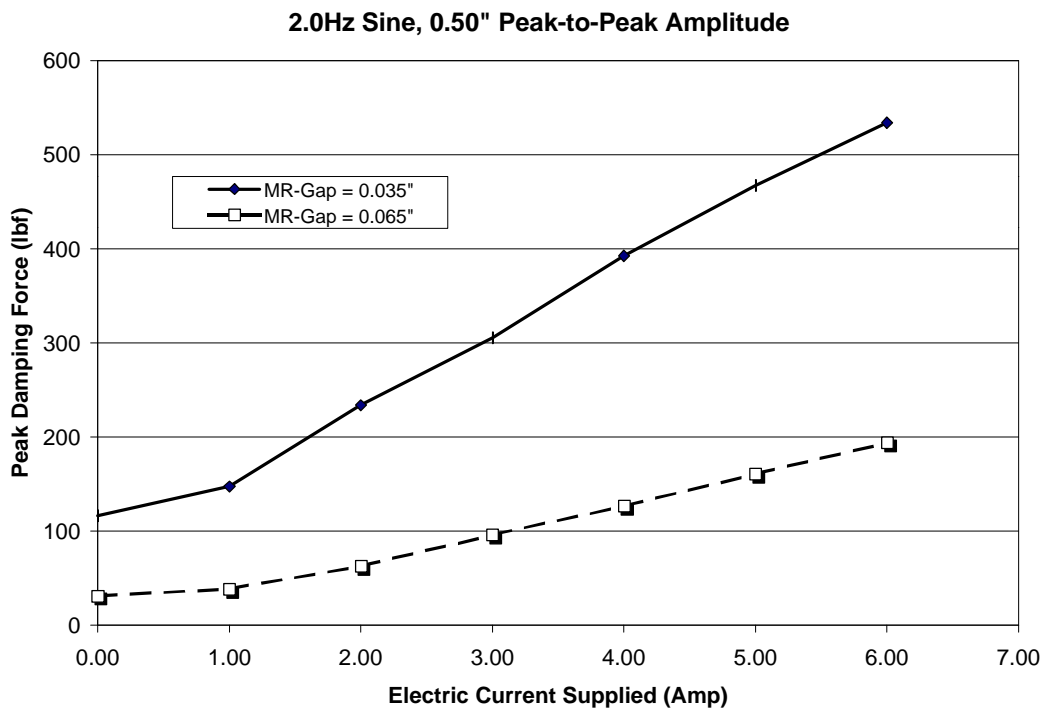


Figure 2 Peak Damping Force as a Function of Electric Current Supplied for Two Separate Orifice Sizes

THE ELECTROMAGNETIC CIRCUIT

One benefit of using MR fluid for varying damping force in lieu of a mechanical method is in device response time: the time required to change *apparent viscosity* of MR fluid is far less than the time a mechanical system requires to vary orifice size [9]. It is the design intent of this MR damper to accommodate feedback control strategies across a broad frequency spectrum. Oftentimes the damper is the limiting factor achieving the highest bandwidth of control, typically due to the device's time response. Typically, an MR fluid device's time response is limited to the time response of the electromagnetic circuit that creates the required flux density within the MR-gap. The design challenge exists in creating a DC electromagnetic circuit that can generate sufficient flux across the MR-gap in a minimum amount of time.

Time response for an electromagnetic circuit can be modeled as a function of inductance and electrical resistance. This can be expressed as:

$$t = \frac{L}{R} \quad (1)$$

Where t is time response, L is inductance, and R is resistance. Minimizing the L/R ratio reduces time constant of the electromagnetic circuit. However, generating sufficient flux in the MR-gap using a ‘practical’ amount of electrical current, under 6A maximum in this case, requires the existence of a minimum number of coil windings, N [11, 12]. This results in a value of electrical resistance correspondent to the total length of magnet wire required. Only one remaining parameter can be manipulated in order to reduce the time response: the inductance.

As represented in Figure 3, inductance of the coil, L_C , can be represented as [13]:

$$L_C = \frac{4\mu^2 N^2 r^2 K_n}{l} \cdot 10^{-6} \quad (2)$$

whose units are in Henries, with radius in terms of inches. The geometry term, K_n , in Equation (2) is defined as [13]:

$$K_n = \frac{1}{1 + 0.9 \frac{r}{l} + 0.32 \frac{t}{r} + 0.84 \frac{t}{l}} \quad (3)$$

Where r is the mean radius, t is thickness, and l is length of the coil along the centerline. Decrease in inductance results from the manipulation of these area terms. Consider the two images presented in Figure 3 and Figure 4. Figure 4 shows an arrangement of three smaller coils whose sum cross-sectional area is equivalent to the area of the single coil shown in Figure 3. It is assumed that the same number of coils and type of magnet wire is used for both cases, hence equivalent values for electrical resistance. The inductance of the electromagnetic circuit in Figure 3 is calculated directly from Equation (2). Inductance for the series electromagnetic circuit of Figure 4 must account for the effects of mutual inductance in addition to the series addition of three individual coil inductances [5]:

$$L_S = L_1 + L_2 + L_3 \pm 2(M_{12} + M_{23} + M_{13}) \quad (4)$$

Where L_S is the summed inductance, L_1 is inductance of the first coil, L_2 the second, and L_3 the third. M_{12} is mutual inductance for the interaction between the first and second coil, M_{23} is mutual inductance for the interaction between the second and third coils, and M_{13} is mutual inductance of the external two coils. The plus/minus sign before the mutual inductance terms indicates that coupling is either additive or subtractive, depending on the connection polarity.

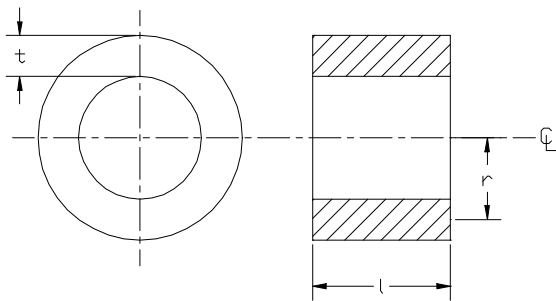


Figure 3 Cross-sectional view of solenoid coil

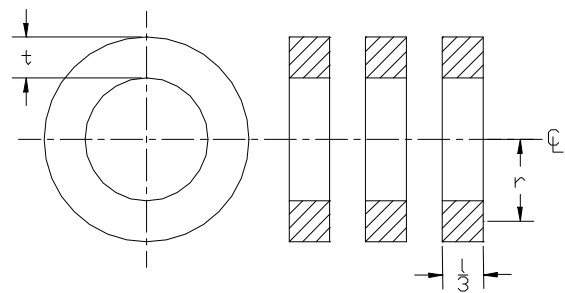


Figure 4 Cross-sectional view of 3 coils in series

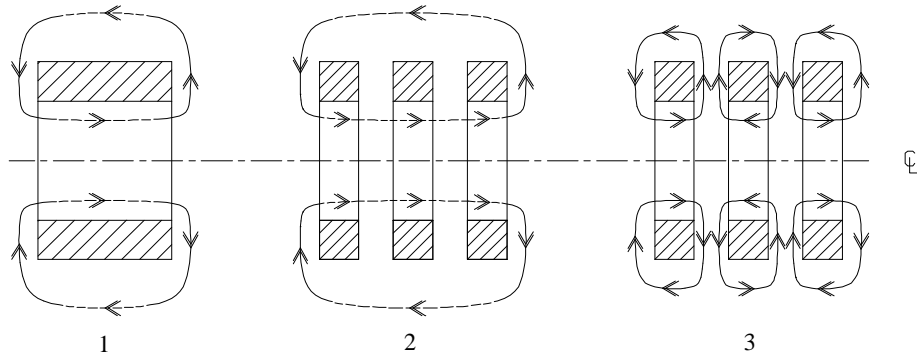


Figure 5 Flux path illustrations for three different coil configurations. The polarity (or direction of wind) of coils in # 3 alternates, while in #2 the polarity is the same, hence different flux paths.

Figure 5 illustrates the difference in connection polarity. Coil configuration #1 has flux lines that flow around the single coil. Coil configurations #2 and #3 represent two three-coil arrangements with similar characteristics except for polarity. Configuration #2 illustrates the flow of flux around three coils with windings in the one direction relative to the centerline. Configuration #3 illustrates the flow of flux around three coils whose winding orientations alternate for each coil. The main difference between the two configurations is the length of the flux paths. The benefit of the coil arrangement on configuration #3 is that the overall inductance of the circuit is much lower than the previous two cases; the mutual inductances are subtracted from overall inductance, hence:

$$\therefore L_{\#3} \ll L_{\#1} \quad \text{and} \quad \therefore L_{\#3} \ll L_{\#2} \quad (4)$$

The result is a comparatively shorter time response with configuration #3 than with configurations #1 or #2. One issue of concern with generating smaller local flux paths such as those found in configuration #3 is the usefulness of the flow of magnetic flux in terms of generating the desired MR-effect. The MR-gap of the MR damper used in this research takes this arrangement into account and delivers the required performance in addition to the benefit of the reduced time response.

RESULTS

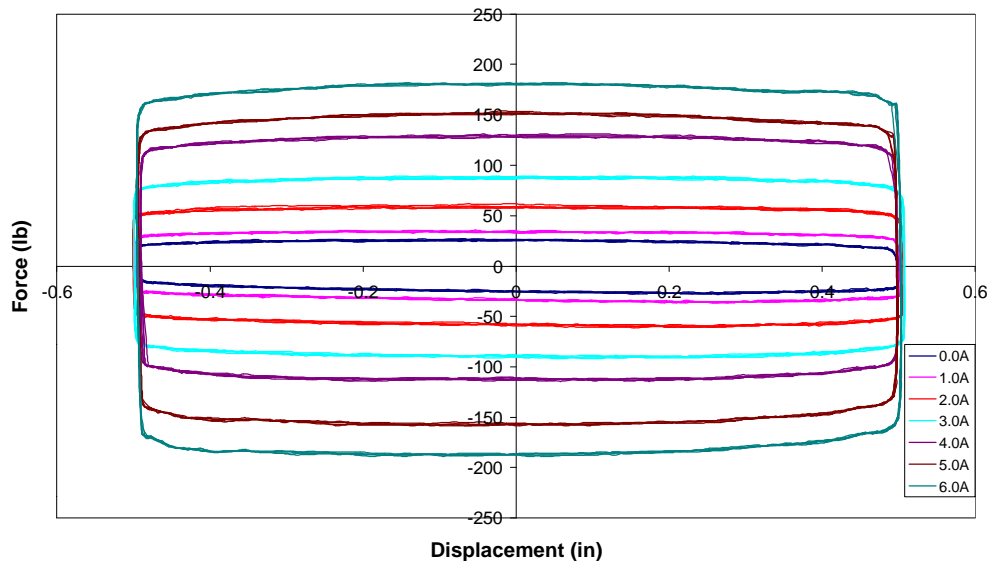


Figure 6 Force versus displacement for 1.0Hz, 0.5" peak for current values of 0.0A to 6.0A (gap height = 0.065")

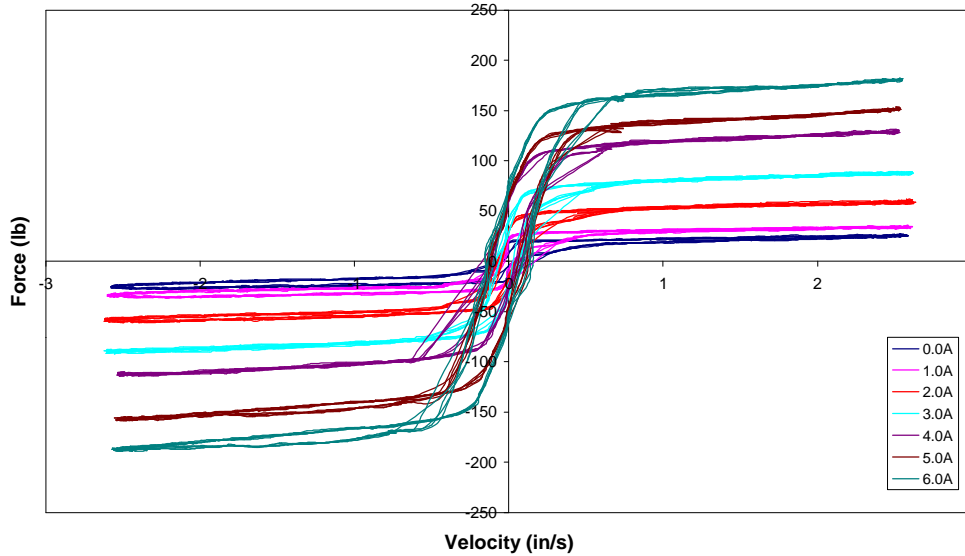


Figure 7 Force vs velocity for 1.0Hz, 0.5" peak for current values of 0.0A to 6.0A (gap height = 0.065")

Figure 6 and Figure 7 are force versus displacement and force versus velocity graphs, respectively, of the MR Damper developed for this research. Seven curves are overlaid in each plot, corresponding to different values of electrical current applied, from 0.0A to 6.0A in increments of 1.0A. The nature of this data is typical to what is measured throughout the range of test points explored. It is evident in the force versus displacement graph that this MR damper provides consistent controllability of damping throughout the current range. Figure 8 is a graph illustrating the peak damping force for the range of current values tested. The dashed line shows damping force for the range of currents supplied at maximum piston velocity, approximately 12.6in/s. The solid line shows damping force the range of currents supplied at the minimum piston velocity tested, approximately 0.39in/s. It is evident that with this design, peak damping forces are more a function of electric current applied than piston velocity. Peak damping forces vary only by an average of 27lbf between minimum and maximum piston velocity.

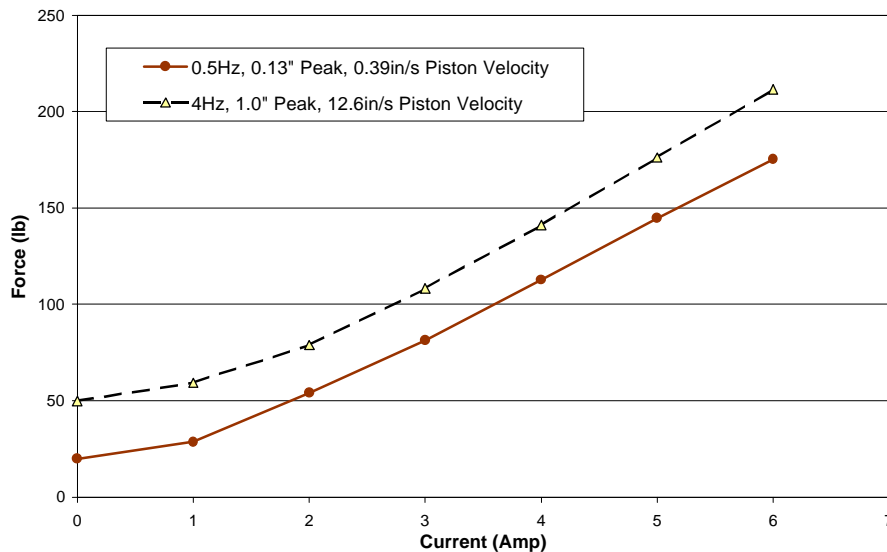


Figure 8 Average peak damping force values as a function of Current for minimum and maximum piston velocities tested

3-PARAMETER SEMI-ACTIVE MR ISOLATION

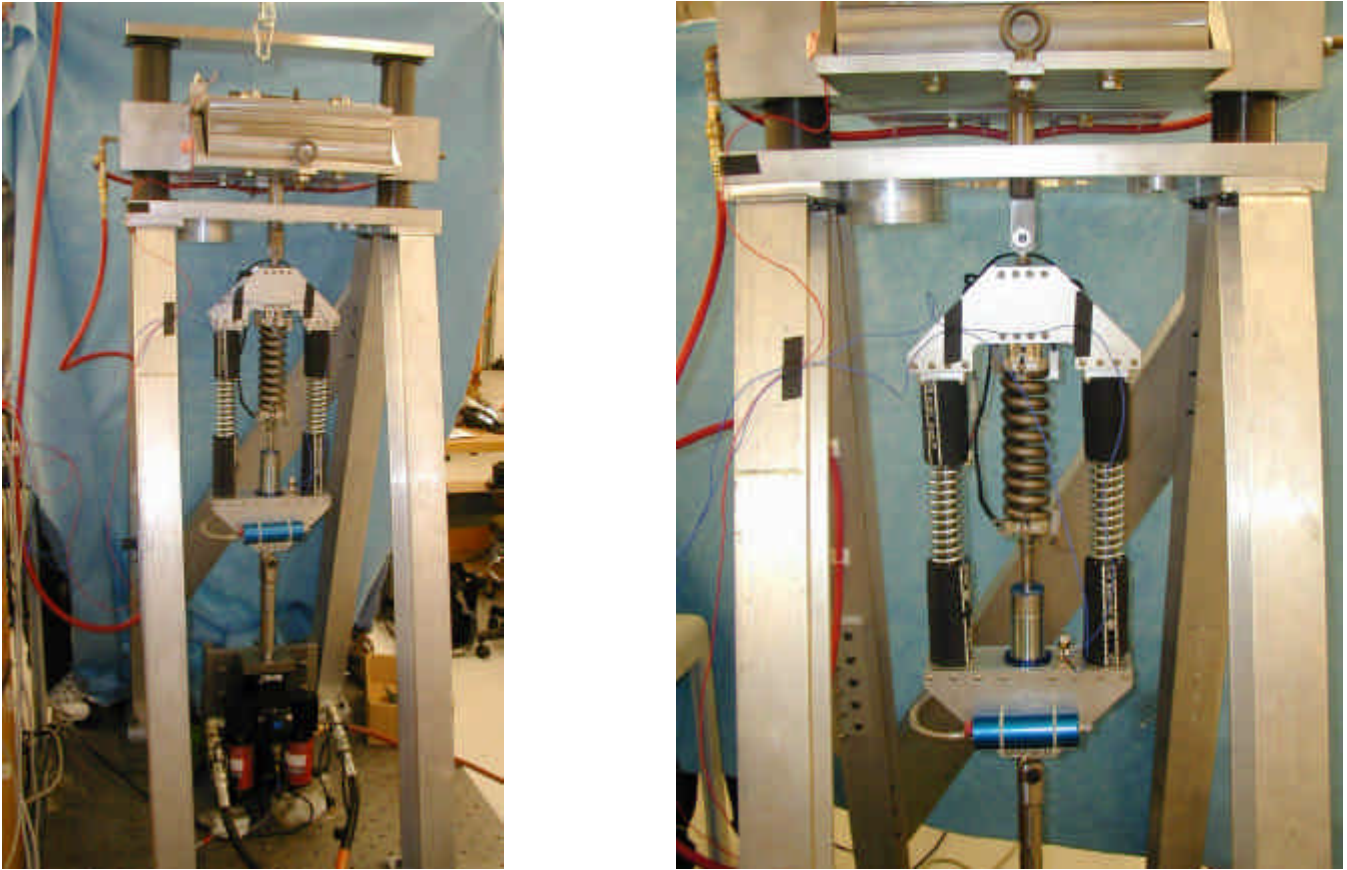


Figure 9 Two views of the MR damper integrated into a 3-parameter isolator and test setup. Base excitation is transmitted across the isolator; base, payload & piston accelerations are measured

The images of Figure 9 show one current application of the MR damper technology mentioned in this research. The test damper is integrated into a three-parameter isolator scaled to the payload mass and isolation requirements of the research. The function of the isolator is to dynamically vary the isolation frequency from 1Hz to 3Hz. Acceleration of the piston relative to the cylinder is integrated digitally and input to a DSP-driven control scheme to actively modulate the contribution of the series spring to the overall isolation stiffness. A hydraulic actuator produces base excitation; a scaled simulation of anticipated Space-Based Laser inputs in this case. Single-degree-of-freedom motion is constrained for both isolator and payload, with the payload utilizing air bearings to eliminate friction concerns during motion. Testing is ongoing, and results will be reported separately. A variant of this technology is currently proposed for two other applications with different stroke and different bandwidth requirements.

CONCLUSIONS

New magnetorheological fluid damper technology has been developed at CSA Engineering. It is designed for portability to a wide variety of research and development applications, while being inexpensive to construct, service and rebuild. The electromagnetic circuit within the piston is capable of a time response that supports high bandwidth, semi-active control. Characterization testing of the device for different gap heights has proven to deliver a broad range of baseline damping force with minimal changes of gap height.

It is evident through the device's successful performance that this technology is feasible and meets the goal of providing a 'whole approach' MR solution. It is of simple construction, it utilizes a coil configuration that delivers a desirable time

response, zero-field damping adjustability works for a broad range of damping needs, and the dynamic force range due to the MR-effect is diverse and linearly proportional throughout its range.

ACKNOWLEDGEMENTS

A portion of the work completed and currently underway was funded by a SBIR Phase 1 research grant provided by the Ballistic Missile Defense Organization, Dr. Benjamin Henderson, technical monitor. The author would like to acknowledge Dr. Pradeep Phule of the University of Pittsburgh for providing MR fluid. The author would also like to Acknowledge CSA Engineering's IRAD (Internal Research and Development) program for providing funding for hardware development and testing.

REFERECNES

1. F. Gordaninejad and S.P. Kelso, "Magneto-rheological fluid shock absorbers for HMMWV," *Proceedings of SPIE Conference on Smart Structures and Materials, Paper No. 3989-21*, Newport Beach, CA, March, 2000.
2. Updated 10 November 2000
3. Lord Materials Division, "Designing with MR Fluids", *Engineering Note*, Lord Corporation, Thomas Lord Research Center, Cary, NC, November 1999.
4. Kelso, S. P. and Gordaninejad, F., "Magneto-Rheological Fluid Shock Absorbers for Off-Highway, High-Payload Vehicles," *Passive Damping and Isolation, Proceedings of the 1998 SPIE Conference on Smart Materials and Structures*, Ed. by L. Porter Davis Vol. 3672 pp. 44-54, 1999.
5. T.A. Bowland, *Electrical Circuit Formulae*, p.5 BOWest Pty Ltd, 1998.
6. M.R. Jolly, J.D. Carlson and J.W. Bender, "Properties and applications of commercial rheological fluids," *SPIE 5th Annual International Symposium on Smart Materials and Structures*, San Diego, CA, 15 March, 1998.
7. F. Yeaple, *Fluid Power Design Handbook*, Third Edition, p. 683, Marcel Dekker, Inc., New York, 1996.
8. Carlson, J. D., Catanzarite, D. M. and St. Clair, K. A., "Commercial Magneto-Rheological Fluid Devices," *Proceedings of the 5th International Conference on ER Fluids, MR Fluids and Associated Technology*, U. Sheffield, UK, pp. 20-28, 1995.
9. Barak, P., "Design and Evaluation of an Adjustable Automatic Suspensions," SAE Paper No. 890089, 1989
10. R. W. Phillips, "Engineering applications of fluids with a variable yield stress," *Ph.D. Dissertation*, University of California, 1969.
11. J. A. Wagner, "The Shorted Turn in the Linear Actuator of a High Performance Disk Drive", *Transactions on Magnetics*, Sperry Univac, Santa Clara, California, and San Jose State University, San Jose, CA, March 29, 1982.
12. M. A. Plonus, *Applied Electromagnetics*, p.221 McGraw Hill Book Company, New York, 1978.
13. V.G. Wellsby, *The Theory and Design of Inductance Coils*, p.27 & 165, Macdonald & Co., (Publishers) Ltd., circa 1952